

Citation: Hirt C. and Seeber, G. (2007) High-Resolution Local Gravity Field Determination at the Sub-Millimeter Level using a Digital Zenith Camera System. In: *Proceed. Dynamic Planet, Cairns 2005*, IAG Symposia 130 (ed. P. Tregoning und C. Rizos), 316-321.

High-Resolution Local Gravity Field Determination at the Sub-Millimeter Level using a Digital Zenith Camera System

Christian Hirt and Günter Seeber

Institut für Erdmessung, Universität Hannover, Schneiderberg 50, 30167 Hannover, Germany

E-mail: hirt@mbox.ife.uni-hannover.de Fax: +49 511 762 4006

Abstract. During the last years the observation of vertical deflections experienced a revival due to the development of state-of-the-art Digital Zenith Camera Systems in Zurich and Hanover. Other than analogue instruments of geodetic astronomy, the new digital observation systems provide vertical deflection data very fast and highly-accurate. One main application for these instruments is the precise gravity field determination in local areas applying the classical method of astronomical leveling.

This paper presents preliminary results of an ongoing local gravity field survey carried out in a test area near Hannover in Northern Germany. Here, a subterranean salt deposit influences the fine structure of the gravity field. At the Earth's surface a profile was established with densely arranged stations (50 m spacing). At 131 stations high-precision vertical deflection data has been collected using the Hanover Digital Zenith Camera System TZK2-D. Based on extensive instrumental calibration and the highly redundant data acquisition at each station, an unprecedented accuracy level of about $0''.08$ is reached for the deflection data.

The local equipotential profile is directly obtained through integration of vertical deflections in the course of the profile. Error propagation shows that the variations of the local gravity field are determined at an accuracy level of $0.1 \frac{mm}{\sqrt{km}}$ required for example in engineering projects (linear accelerators). As a conclusion the study demonstrates that Digital Zenith Cameras are ideal instruments for accessing the sub-millimeter accuracy domain for gravity field studies in local areas.

Keywords. Digital Zenith Camera System, vertical deflection, astronomical leveling, gravity field fine structure, least squares collocation

1 Introduction

Over the past five years, considerable advances have been made in the field of geodetic astronomy by the development of Digital Zenith Camera Systems (DZCS) in Zurich and Hannover. Due to the application of digital imaging and a high degree of au-

tomation, this new type of instrument provide the deflection of the vertical very fast at an extremely low noise level. Using a DZCS, the complete observation procedure of determining vertical deflections at a single station lasts 20-30 min including instrumental set up, time for 50 single observations and data processing. If compared to techniques from the analogue era of geodetic astronomy, today vertical deflection data can be provided with utmost efficiency and accuracy.

These benefits led to an intensive use of DZCSs in local and regional gravity field determinations in the recent time. At some 100 stations vertical deflections have been observed, e.g. in Switzerland 2003 for regional gravity field modeling (Müller et al. 2004; Brockmann et al. 2004), in Northern Germany (Hirt 2004; Hirt et al. 2004), in further campaigns in Bavaria and Portugal 2004, Switzerland and Greece 2005 (currently yet unpublished).

A substantial field of application for DZCSs is the highly-precise determination of the gravity field at local scales. Applying the traditional method of astronomical leveling, information on the local gravity field can be easily derived. The spatial resolution and the accuracy of the gravity field profile are a function of station spacing which can be adapted to the problem to be solved. Shortening the station spacing leads to a nearly unlimited spatial resolution and opens the possibility to access the sub-millimeter accuracy level over distances of a few kilometer. An initial study showing the potential of astronomical leveling carried out with a DZCS has been already presented by Hirt and Reese (2004).

While the general characteristics of the Earth's gravity field are well-known for the most part of its spectrum, there is currently only less knowledge available regarding very high-frequent fine structures with wavelengths in the kilometer-range or even smaller. This is the point where this contribution enters into: The aim of this paper is to present preliminary results of an ongoing astrogeodetic high-resolution local gravity field survey carried out above a salt-dome in Northern Germany. The derived data set consists of 131 vertical deflection stations with a close spacing of 50 m thus allowing to obtain empi-

rical information on the high-frequent portion of the local gravity field.

The chosen test area near Hannover is completely even and situated at a height of approximately 40 m above mean sea level. The astrogeodetic gravity field profile is referred to this height as it is directly computed from the deflection data. The impact of the curvature of the plumb line is assumed to be rather small and neglected in the presented data analysis. The derived gravity field profile located in observation height is subsequently called "equipotential profile" with the corresponding variable ΔN . It directly corresponds to the shape a free water surface follows. Strictly spoken neither the local geoid nor the quasigeoid is obtained although the equipotential profile derived approximates the corresponding geoid profile very well due to the small elevation of the area. General results regarding the fine structure are not depending on this proceeding. It should be emphasized that the results presented have preliminary character as the gravity field survey is still ongoing.

2 The Digital Zenith Camera System TZK2-D

The Digital Zenith Camera System TZK2-D developed and operated by the Institut für Erdmessung, University of Hannover is used as sensor for this local gravity field study. In this paper it is only briefly presented since its characteristics have already been published (cf. Hirt 2004, Hirt and Bürki 2002). The TZK2-D consists of two major components. Firstly, a digital image sensor (CCD) is applied for the astrogeodetic determination of the plumb line (Φ, Λ). For the data processing the highly-accurate star catalogue UCAC (Zacharias et al. 2004) serves as celestial reference. The fully-automated data processing from image data to vertical deflections is done with the Hannover astrogeodetic processing system AURIGA (cf. Hirt 2004). Secondly, a GPS-receiver is used for precise timing and positioning (ellipsoidal coordinates φ, λ). Vertical deflections (ξ, η) are obtained by combining both components:

$$\xi = \Phi - \varphi \quad \eta = (\Lambda - \lambda) \cos \varphi. \quad (1)$$

In early 2005, the TZK2-D was undergoing a thorough reworking by installing a set of motors in order to automatically perform necessary motions during the instrumental set up (leveling and focusing) and observation procedure (camera rotation). These technical enhancements resulted in a complete automation of observation so that the determination

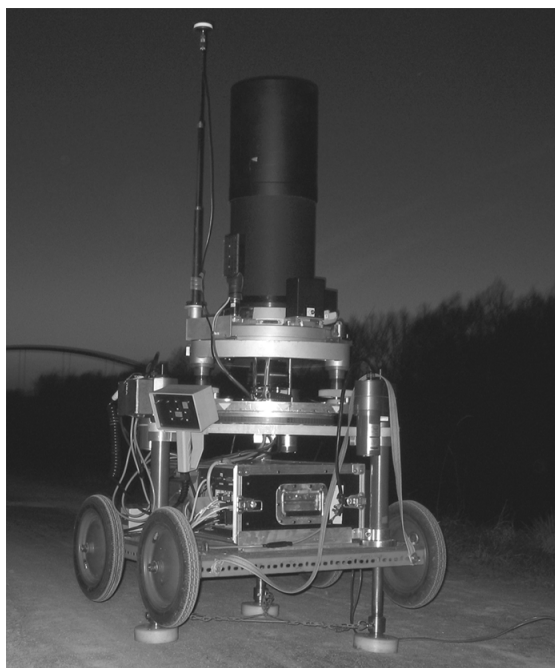


Figure 1. The Hannover Zenith Camera System TZK2-D in action above the salt dome

of vertical deflections now is a "one-mouse-click-application".

A recently developed and tested observation strategy eliminates the influence of instrumental zero-offset variations on the deflection data. This improvement has increased the accuracy level of the deflection data from $0''.10 - 0''.15$ (derived in Hirt et al. 2004) significantly in the unprecedented range of $0''.05 - 0''.10$ ¹.

3 Project Area

As a test area the salt dome "Bokeloh", forming a part of the salt structure "Steinhuder-Meer-Linie" near Hannover in Northern Germany, has been selected. The salt dome creates an extended subterranean geophysical anomaly as its density contrasts from the surrounding sediment layers. Due to the geometrical extensions of the salt dome (width of approximately 1 km, length of 12 km, depth of 3 km) and complexly folded neighbouring sediment layers the test area is ideal for studying the local gravity field fine structure. Small disturbances of the local gravity field may be expected. Since the salt dome "Bokeloh" is presently exploited by the German min-

¹The accuracy obtained in practice is essentially a function of the number of single observations and the presence of refraction anomalies during observation. An accuracy of about $0''.05$ is usually reached on the basis of about 100 or more repeated observations.

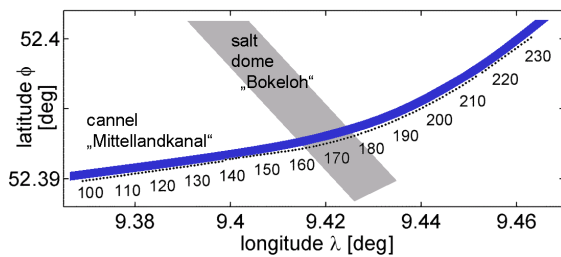


Figure 2. Course of the astrogeodetic profile and approximate location of the salt dome. Note the different scales of the longitude- and latitude axis.

ing company "K+S GmbH" the geometrical position of the salt structure is well known on the basis of exploration data (cf. Sessler and Holländer 2002). However, precise three-dimensional information on the mass and density distribution in the neighbourhood of the salt dome is not available.

In order to sample the local gravity field with high-resolution, a profile with a length of 6.5 km consisting of densely arranged stations with a spacing of 50 m has been set up at the Earth's surface. Due to aligning the profile line to the course of the "Mittel-landkanal" (a canal in East-West-direction) a relatively smooth profile course was achieved (Figure 2).

4 Astrogeodetic Observations

Within thirteen clear nights in spring 2005 a total of 150 observation series have been carried out at 131 stations using the TZK2-D. Because a single observation series of the deflection of the vertical consists of 50 repeated observations, the derived astrogeodetic (ξ, η) data set is basing on a total of approximately 6700 single solutions². According to the efficiency aspects mentioned in section 1, in average two stations have been occupied per hour. Depending on the length of night, within most nights deflection data has been collected at 10-17 different stations. A first accuracy estimation is obtained from the residuals of double measurements in different nights which is in the order of $0''.08$ for ξ and η . These figures underline the utmost efficiency and accuracy of modern astrogeodetic observation systems like the TZK2-D.

5 Data Processing and Analysis

As a first step of data processing the double observations carried out at identical stations have been averaged. As a second step the geometrical course of the profile has been slightly smoothed in order to sup-

²A single observation of the deflection of the vertical is composed of a pair of digital images. Since a single zenithal image contains 20-30 stars in average, a total of more than 300.000 processed directions to stars contribute to the (ξ, η) data set (!).

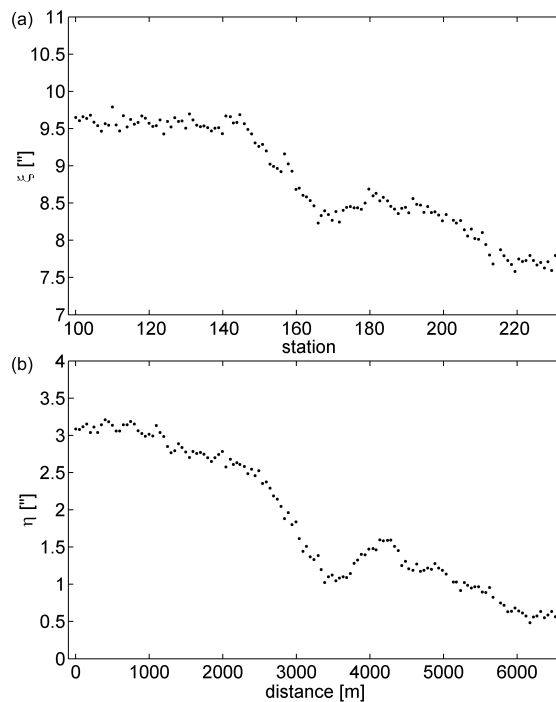


Figure 3. Vertical deflections (ξ, η) in the course of the astrogeodetic geoid profile crossing the salt dome "Bokeloh"

press small peak-structures in the equipotential profile.

5.1 Analysis of the Deflection Data

The (ξ, η) - data set obtained is depicted in Figure 3 as a function of distance. In the profile's course a variation of about $2''$ (ξ) and $3''.5$ (η) is visible. Both components show local minima located approximately in the middle of the profile (station range 160-180) where the main part of the salt dome is located. The very low noise level of the data sets is clearly visible in both figures. Applying the method of least squares collocation for separating signal from noise (cf. section 5.2), the noise level of the deflection data is found to be about $0''.08$ (ξ) and $0''.07$ (η)³. As such it corresponds to the initially made accuracy estimation yielded by double observations (cf. section 4).

5.2 Computation and Analysis of the Equipotential Profile

Applying the well-known classical formulae of astronomical leveling, the equipotential profile ΔN is

³However, the noise of the ξ -component is obviously not normally-distributed as seen by locally strong correlated parts (e.g. stations 150-160 or stations 210-220). This is most likely due to the presence of small, very local refraction anomalies which may occur perpendicular to the profile over the canal's water surface.

obtained. Using the average of the vertical deflections at every pair of adjacent stations P_i and P_{i+1} , the vertical deflection ε_i

$$\varepsilon_i = \frac{\xi_i + \xi_{i+1}}{2} \cos \alpha + \frac{\eta_i + \eta_{i+1}}{2} \sin \alpha \quad (2)$$

is obtained being the tilt of the equipotential profile in azimuth α of the connecting line between stations P_i and P_{i+1} (according to Torge 2001, pp 294-300). The equipotential profile ΔN (= height difference between P_i and P_n) is obtained by integrating single height increments $\varepsilon_i \cdot s_i$ from the beginning (station no. 100) to the end (station no. 231) of the profile:

$$\Delta N = - \sum_{i=100}^{i=230} \varepsilon_i \cdot s_i. \quad (3)$$

Figure 4 shows the course of the vertical deflection component ε . The salt dome's signal of about $1''$ is clearly visible in the range of stations 160-180. Contrary to the relatively smooth course from station 130 to 231 the range between station 100 and 130 reveals correlated noise which is certainly not coming from the Earth's gravity field⁴. The result of the computation of the equipotential profile is depicted in Figure 5. The height of the equipotential profile changes by approximately 10 cm over a distance of 6.5 km.

In order to extract information on the fine structure contained in the ΔN data the method of least squares collocation (LSC) can be applied which is described in detail by Moritz (1980). The general form of LSC observation equation reads as (Torge 2001, p. 303):

$$\mathbf{l} = \mathbf{A}\mathbf{x} + \mathbf{s} + \mathbf{n}. \quad (4)$$

For the analysis of astrogeodetic profile measurements, \mathbf{l} is the observation vector comprising the gravity field quantities ΔN_{1i} in the course of the profile:

$$\mathbf{l}^T = [\Delta N_{11}, \Delta N_{12}, \dots, \Delta N_{1n}] \quad (5)$$

and \mathbf{x} is the parameter vector with profile distances from 0 m to about 6500 m. The product $\mathbf{A}\mathbf{x}$ expresses the deterministic part, e.g. a straight trend line as first approximation. The signal vector \mathbf{s} and the noise vector \mathbf{n} are random parts of the observation vector \mathbf{l} . Whereas the signal vector \mathbf{s} includes correlated (quasi-deterministic) parts, the latter usually represents observation errors, namely noise. The

⁴The noise reflects variations of instrumental zero offsets which are not adequately eliminated during the observation procedure at the very beginning of the campaign.

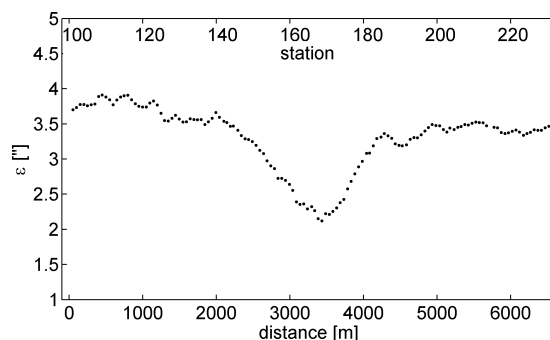


Figure 4. Vertical deflection component ε in the course of the astrogeodetic geoid profile. Averaging of the deflections from neighboured stations yields to a smoother profile course if compared with ξ and η (Fig. 3).

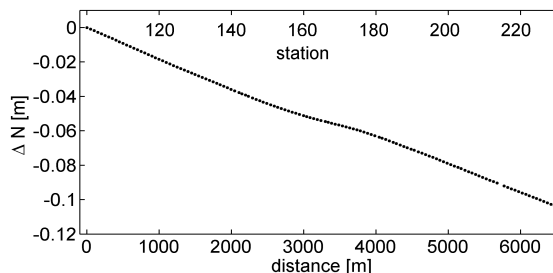


Figure 5. Equipotential profile ΔN

stochastic properties are described by the signal covariance matrix \mathbf{C} and the noise covariance matrix \mathbf{D} . For the computation of \mathbf{x} , \mathbf{s} and \mathbf{n} the reader is referred to Moritz (1980) or Torge (2001). In LSC, two parameters essentially control the separation of signal \mathbf{s} and noise \mathbf{n} : At first, the ratio between a priori standard deviations σ_s and σ_n for signal and noise is necessary. Secondly, the covariance function $\text{cov}(\mathbf{l}, \mathbf{l}')$ containing information on the autocorrelation between neighboured stations P and P' is required for the determination of the signal covariance matrix \mathbf{C} . As the LSC results are relatively insensitive to the chosen covariance function, an exponentially decreasing correlation function can be used with a correlation length of about 1 km.

Instead of an estimated signal-to-noise-ratio of about 10 a smaller value of 1 has been used for collocation. This has the advantage that interesting fine structures with small amplitudes are separated from the main signal of the equipotential profile. Following that way, the information contained in \mathbf{l} with amplitudes of a few 0.1 mm or less is included in the noise vector \mathbf{n} and becomes visible.

Figure 6 (a) shows the filtered equipotential profile. It is equivalent to the difference between the ob-

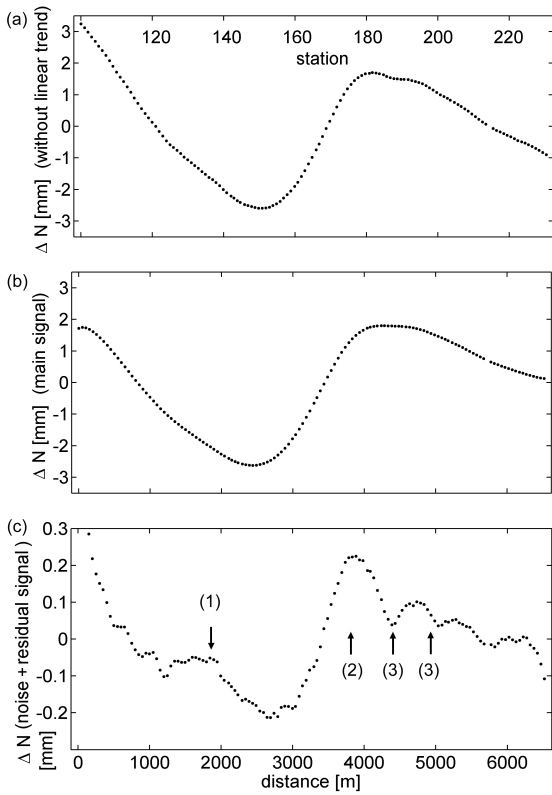


Figure 6. Equipotential profile. In subfigure (a) the filtered profile is depicted ($= \mathbf{l} - \mathbf{A}\mathbf{x} = \mathbf{s} + \mathbf{n}$). The signal part \mathbf{s} is displayed in subfigure (b). Residual signal parts (fine structure) and observation errors are contained in the noise vector \mathbf{n} illustrated in subfigure (c).

observation vector \mathbf{l} and the deterministic part $\mathbf{A}\mathbf{x}$. The latter corresponds to the long-wave regional part of the gravity field. Subtracting the noise vector \mathbf{n} , the signal vector \mathbf{s} is obtained (Figure 6 (b)). A wave-like structure forms the dominant part of the graph with an amplitude of about 2 mm and an estimated length of 5 km. As such it reflects the local mass distribution. The noise vector \mathbf{n} as *residual profile* is shown in Figure 6 (c) as the most interesting depiction. This vector contains measurement noise and highly correlated patterns which basically may come from atmospheric refraction anomalies and inhomogeneous subterranean mass distribution. The visible features may be explained as follows:

(1) The presence of atmospheric refraction anomalies leads to physical correlation of neighbored stations if measured during the same night. Mean amplitudes of this effect come usually close to some $0''01$ (estimation based on results of repeated observations in Hannover 2005). However, extreme weather situations may cause refraction anomalies estimated to be in the order of $0''1$. Consequently, for

the analysis of the residual profile refraction anomalies are not negligible. For example the correlated point patterns occurring in the station range 135-140 (cf. arrow in Figure 6) are believed to come from refraction anomalies.

(2) Within the station range 160-210 various fine structure features with different characteristics are visible. The most striking fine structure is visible within the station range 170-185 (estimated amplitude 0.1 mm, half wavelength 800 m). A first comparison with detailed geological data (courtesy K+S GmbH) reveals a strong local correlation with subterranean sediment layers. As such this structure most likely reflects the very local mass distribution.

(3) Even finer structures are visible from station 185 to 195 (amplitude 0.05 mm, half wavelength 400 m) and 195 to 210 (0.02 mm, 350 m). However, it is not clear where these structures come from. Currently it can neither be excluded nor confirmed whether these patterns are also mirroring very local mass anomalies. As a future task further repeated astrogeodetic measurements will be carried out in order to find out more about these interesting structures.

On the basis of Figures 6 (a) - (c) it can be concluded that the sediments located at both sides of the salt dome have different densities and are not homogeneously distributed.

5.3 Accuracy of the Equipotential Profile

The accuracy $\sigma_{\Delta N}$ of the equipotential profile is a function of the observation accuracy σ_ε , station spacing ds and number of stations n . According to the derived formulae described in Hirt and Reese (2004) the accuracy $\sigma_{\Delta N}$ in [mm] is given by

$$\sigma_{\Delta N} = \sqrt{n-1} \cdot 4.8 \cdot ds \cdot \sigma_\varepsilon \quad (6)$$

where σ_ε is introduced in [$''$] and ds in [km]. Applying equation 6 the standard deviation $\sigma_{\Delta N}$ is found to be about $0.09 \frac{mm}{\sqrt{km}}$ for an observation accuracy of about $0''08$ (cf. Table 1). Even a lower observation accuracy of $0''1$ still yields an accuracy being in the order of $0.1 \frac{mm}{\sqrt{km}}$. The sub-millimeter level is also clearly achieved for profile lengths up to 10 km. These figures underline that astronomical leveling can provide local gravity field information on an unprecedented accuracy level. Anyway, remaining systematic errors due to refraction are not yet taken into account. Therefore adequate consideration of refractivity (e.g. modeling or reduction by observation techniques) remains as future task.

σ_ε ["]	Total length of profile [m]				
	50	600	1000	6500	10000
0.05	0.012	0.042	0.054	0.139	0.172
0.07	0.017	0.059	0.076	0.194	0.241
0.08	0.019	0.067	0.087	0.222	0.275
0.10	0.024	0.084	0.109	0.278	0.344
n	2	13	21	131	201

Table 1. Accuracy $\sigma_{\Delta N}$ as a function of profile length and observation accuracy σ_ε for a station spacing of 50 m.

6 Conclusion and Outlook

In this paper preliminary results of a high-resolution local gravity field survey have been presented using the Digital Zenith Camera System TZK2-D for observation of vertical deflections. The sub-millimeter accuracy level of about $0.1 \frac{mm}{\sqrt{km}}$ has been reached for the equipotential profile due to the unsurpassed low noise level of the deflection data of about $0''08$ and the very dense station spacing of 50 m. Analysis of the gravity field profile using least squares collocation indicates the existence of very short-wavelength fine structure with amplitudes of some 0.02 mm and wavelengths in the order of 1 km.

Having highly-resolved data opens the possibility to a better understanding of the finest components of the gravity field. Besides geodesy, geology and geophysics could benefit from new astrogeodetic data sets like the presented one as data inversion can provide precise information on the density distribution of the subterranean masses. Furthermore, even highest accuracy requirements in engineering projects can benefit from astronomical leveling using digital instrumentations. E.g., the alignment of new linear accelerators require exceptionally precise information on the geometry of the gravity field at an level of about 0.1 mm per 600 m (cf. Becker et al. 2002; Schlösser and Herty 2002). As seen from Table 1, astronomical leveling basically meets this requirement.

The presented study shows that some work remains to be done in the future. In general, attention has to be laid on the appropriate consideration of refraction anomalies. With respect to the validation of geoid and quasigeoid profiles, the role of the curvature of the plumb line respectively normal line should be discussed in detail. In particular, selected stations of the equipotential profile (e.g. station range 160-210) should be observed repeatedly using the system TZK2-D. This new data set to be obtained under completely different atmospheric conditions could help to answer the question whether the fine structure features with amplitudes of a few 0.01 mm

which are visible in the data (section 5.2) come from the Earth's gravity field or from the refraction field.

7 Acknowledgement

The application of the Digital Zenith Camera System for gravity field determination is supported by the German National Research Foundation DFG. The authors are grateful to the students Ilka Rehr, Niels Hartmann, Eiko Münstedt and Rene Gudat for their unrelentless and engaged support of the astrogeodetic measurements. Dr. Holländer (K+S GmbH) is acknowledged for providing detailed geological data.

References

- Becker, F., Coosemans, W. und Jones, M. (2002). *Consequences of Perturbations of the Gravity Field on HLS Measurements*. Proc. of 7th Int. Workshop on Accelerator Alignment (IWAA): 327-342, SPring-8, Japan.
- Brockmann, E., Becker, M., Bürki, B., Gurtner, W., Haefele, P., Hirt, C., Marti, U., Müller, A., Richard, P., Schlatter, A., Schneider, D., and Wiget, A. (2004). *Realization of a Swiss Combined Geodetic Network (CH-CGN)*. EUREF'04 Symposium of the IAG Commission 1 - Reference Frames, Subcommittee 1-3a Europe (EUREF), Bratislava, Slovakia.
- Hirt, C. (2004). *Entwicklung und Erprobung eines digitalen Zenithkamerasystems für die hochpräzise Lotabweichungsbestimmung*. Wissenschaftliche Arbeiten der Fachrichtung Geodäsie und Geoinformatik an der Universität Hannover Nr. 253.
- Hirt, C. and Bürki, B. (2002). *The Digital Zenith Camera - A New High-Precision and Economic Astrogeodetic Observation System for Real-Time Measurement of Deflections of the Vertical*. Proc. of the 3rd Meeting of the International Gravity and Geoid Commission of the International Association of Geodesy, Thessaloniki, Greece (ed. I. Tziavos): 161-166.
- Hirt, C. and Reese, B. (2004). *High-Precision Astrogeodetic Determination of a Local Geoid Profile Using the Digital Zenith Camera System TZK2-D*. Electronic Proc. IAG GGSM2004 Meeting in Porto, Portugal. Published also in: CHGeoid 2003, Report 03-33 A (ed. U. Marti et al), Bundesamt für Landestopographie (swisstopo), Wabern, Schweiz.
- Hirt, C., Reese, B., and Enslin, H. (2004). *On the Accuracy of Vertical Deflection Measurements Using the High-Precision Digital Zenith Camera System TZK2-D*. GGSM 2004 IAG International Symposium Porto, Portugal (ed. C. Jekeli et al.), Springer, Heidelberg: 197-201.
- Müller, A., Bürki, B., Kahle, H.-G., Hirt, C., and Marti, U. (2004). *First Results from New High-precision Measurements of Deflections of the Vertical in Switzerland*. GGSM 2004 IAG International Symposium Porto, Portugal (ed. C. Jekeli et al.), Springer, Heidelberg: 143-148.
- Moritz, H. (1980). *Advanced Physical Geodesy*. Wichmann Karlsruhe.
- Schlösser, M. and Herty, A. (2002). *High Precision Survey and Alignment of Large Linear Colliders - Vertical Alignment*. Proc. of 7th Int. Workshop on Accelerator Alignment (IWAA): 343-355, SPring-8, Japan.
- Sessler, W. and Holländer, R. (2002). *Das Kaliwerk Sigmundshall der K+S Aktiengesellschaft*. Veröffentlichungen der Akademie der Geowissenschaften zu Hannover 20: 7-76.
- Torge, W. (2001). *Geodesy, Third Edition*. W. de Gruyter, Berlin, New York.
- Zacharias, N., Urban, S. E., Zacharias, M. I., Wycoff, G. L., Hall, D. M., Monet, D. G., and Rafferty, T. J. (2004). *The Second US Naval Observatory CCD Astrograph Catalog (UCAC2)*. The Astronomical Journal 127: 3043-3059.